LIBRARY Michigan State University



OVERDUE FINES:

25¢ per day per item

RETURNING LIBRARY MATERIALS:

Place in book return to remove charge from circulation records

38 1111

MANGANESE AND PHOTOSYNTHETIC WATER OXIDATION

Ву

JONATHAN EDWARD LAWNICZAK

A THESIS

Submitted to
Michigan State University
in partial fulfillment of the requirements
for the degree of

MASTER OF SCIENCE

Department of Chemistry

ABSTRACT

MANGANESE AND PHOTOSYNTHETIC WATER OXIDATION

by

Jonathan Edward Lawniczak

A recent report described the use of cholic acid and ammonium sulfate to extract a manganese containing enzyme from the water oxidation center of chloroplasts. The effect of cholic acid and ammonium sulfate on manganese involved in photosynthetic water oxidation in chloroplasts is studied using electron paramagnetic resonance spectroscopy. The evidence presented indicates that most of the manganese remains in the membrane. The properties of the manganese left in the membrane following treatment with cholic acid and ammonium sulfate are examined by monitoring the hexaquo Mn²⁺ EPR signal after exposure of the membrane to reagents known to affect manganese in the water oxidation center.

Signal IIf is found in the chloroplast membrane after treatment with cholic acid and ammonium sulfate, indicating the presence of Z, the intermediary between the Photosystem II reaction center and the water oxidation complex. The microwave power saturation profile of Signal II is examined.

.

ACKNOWLEDGEMENTS

I would like to thank Professor Jerry Babcock under whose guidance the research reported here was carried out. In the encouragement and freedom he gave he was the best of teachers. His joyous dedication to the pursuit of knowledge will always be an inspiration to me.

I also thank Professor Charles Yocum for his encouragement and confidence and for his many helpful discussions.

TABLE OF CONTENTS

| LIST | OF | TABLES. Pag . . | <u>e</u> | |
|---------------|----------------------|---|----------------|--|
| LIST | OF | FIGURES | v | |
| ABBREVIATIONS | | | | |
| Α. | 1. 2. 3. 4. | TRODUCTION. The Z scheme. The S states. Mn and oxygen evolution Inhibitors of oxygen evolution. a) Ammonia. b) Hydroxylamine. c) Tris. d) Ca ²⁺ . 1 | 158001 | |
| B. | Mn ² | ² EPR SIGNAL | 3 | |
| C. | AC: | | 122350 0 0 699 | |
| D. | CON | NCLUSION | 6 | |
| REFERENCES | | | | |

LIST OF TABLES

- Table 1. The amount of manganese released by various treatments from chloroplast suspension and from the pellet and the supernatant obtained after treatment of chloroplasts with cholic acid and ammonium sulfate as detected with EPR. Amount of manganese reported in concentration units appropriate to each system. HCl data includes total manganese in sample.
- Table 2. Individual effects of cholic acid and ammonium sulfate on manganese release and oxygen evolution in chloroplasts. p. 37

LIST OF FIGURES

| Figure 1 | The photosynthetic Z-scheme |
|-----------|---|
| Figure 2 | Schematic drawing of the thylakoid membrane showing relative positions of electron chain components |
| Figure 3 | Plot of amount of oxygen released per flash vs. flash number. |
| Figure 4 | Energy transitions for the selection rule, $\Delta M_S = 1$ |
| Figure 5 | Hyperfine splitting of the $\frac{1}{2} \longleftrightarrow -\frac{1}{2}$ transition |
| Figure 6 | EPR spectrum of Mn(H ₂ O) ²⁺ |
| Figure 7 | Effects of increasing concentration of Tricine and Hepes on the EPR signal of 100 μM MnCl ₂ |
| Figure 8 | Calibration curve for the determination of Mn ²⁺ concentration from EPR measurements |
| Figure 9 | Light saturation curve for oxygen electrode |
| Figure 10 | EPR spectra of chloroplast suspension, cholate pellet and cholate supernatant before and after treatment with 1 N HCl |
| Figure ll | Plot of Mn ²⁺ release from the cholate pellet with increasing hydroxylamine concentration |
| Figure 12 | Signal II in the cholate pellet |
| Figure 13 | Microwave power saturation curve for Signal II found in the cholate pellet |

ABBREVIATIONS

Chl Chlorophyll

DPC Diphenylcarbazide

EDTA Ethylenediaminetetraacetic acid

EPR Electron Paramagnetic Resonance

G Gauss

HEPES N-2-Hydroxyethylpiperazine-N'-2-

ethanosulfonic acid

KD Kilodalton

MV Methyl viologen

NADP Nicotinamide adenine dinucleotide

phosphate

NMR Nuclear Magnetic Resonance

PS I Photosystem I

PS II Photosystem II

S Water oxidizing system

Tricine N-tris(hydroxymethyl)methylglycine

Tris (hydroxymethyl) aminomethane

A. INTRODUCTION

Photosynthesis in green plants ultimately is the use of light to drive the reduction of CO_2 and the oxidation of H_2O to form carbohydrates and oxygen as shown in Equation (1):

$$CO_2 + 2H_2O \xrightarrow{h\nu} (CH_2O) + O_2$$
 (1)

where (CH_2O) represents 1/6 of a glucose molecule. Ruben et al. have shown that the molecular oxygen formed comes entirely from water [1]. At pH 7, the formation of O_2 from $2H_2O$ occurs with the release of four electrons and requires an input of 3.2 eV. A photon of absorbed light (680 nm) contains about 1.8 eV [2], i.e., more than one photon is required for water oxidation to occur. In the following sections, we will see that absorption of four photons is necessary for oxygen production and that the photosynthetic apparatus has developed a means of storing the energy of these photons until sufficient energy has been accumulated to oxidize water.

1. The Z-scheme

Figure $\underline{1}$ shows the relation of oxygen formation to other light drive processes in photosynthesis. Commonly

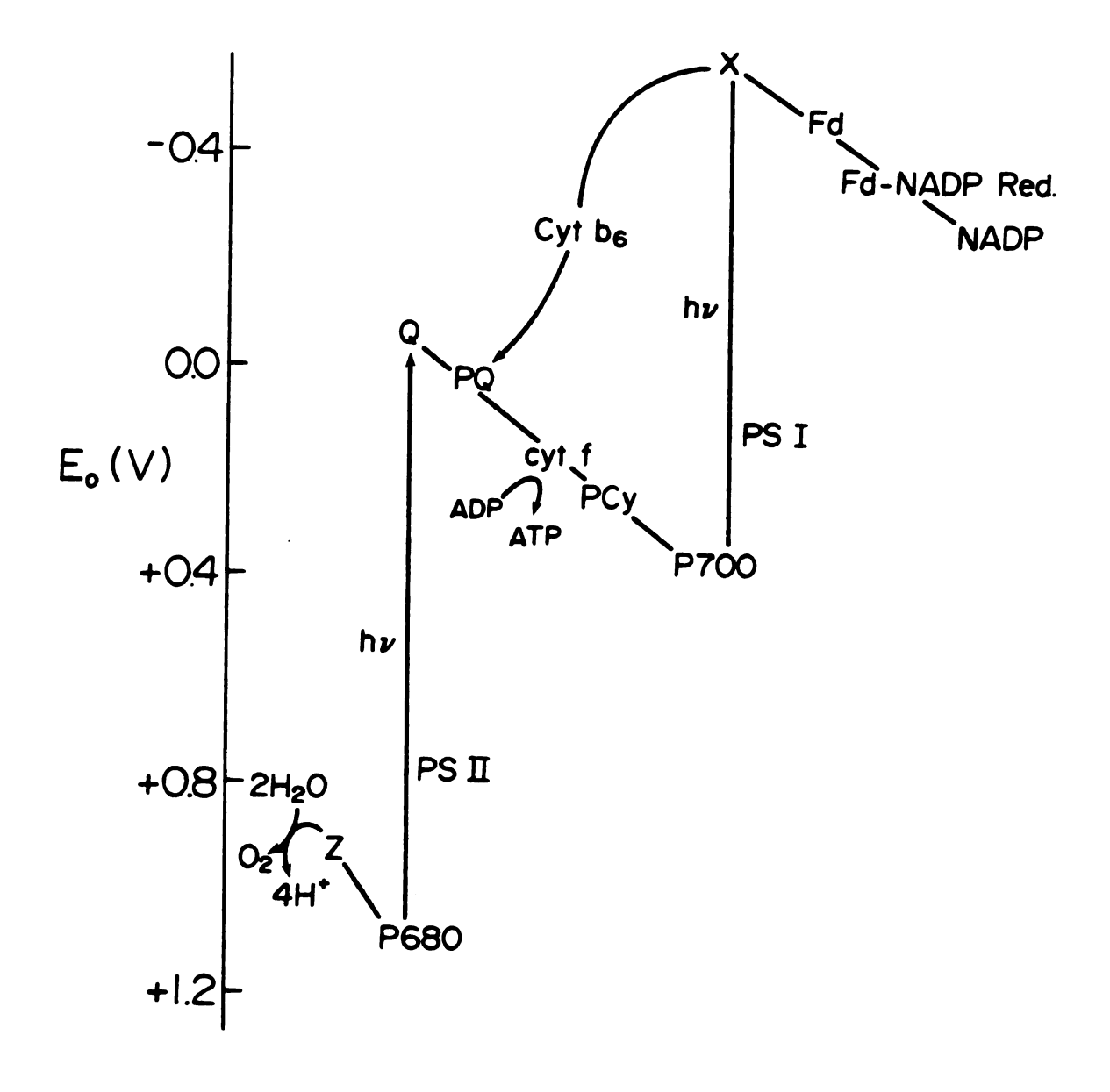


Figure 1. The photosynthetic Z-scheme. P680 is the reaction center chlorophyll and primary electron donor of Photosystem II (PS II). Z is the donor to P680 and is the intermediate between the reaction center and the water oxidation complex. Q is the primary electron acceptor of PS II. P700 is the primary donor of Photosystem I (PS I) and X is the primary acceptor. The two photosystems are connected by the pool of electron carriers, PQ (plastiquinone), cyt f (cytochrome f) and PCy (plastocyanin). PS I is connected to NADPH production by Fd (ferrodoxin) and NADP Red (NADP reductase). From [38].

called the Z-scheme, the diagram follows the electron flow in the chloroplast membrane. Light energy is collected by antennae chlorophyll and channeled to one of the two reaction centers, P680 and P700. The ratio of antennae chlorophyll to reaction center is typically 400/1 [41]. P680, having an absorption maximum at 680 nm, is the reaction center chlorophyll of Photosystem II. Upon absorption of light, this reaction center reaches the first excited singlet state and transfers an electron to the primary acceptor of Photosystem II, called Q. An electron is transferred through the chain of electron carriers which connects the two photosystems to the reaction center of Photosystem I, P700. This chlorophyll a has an absorption maximum at 700 nm. Upon absorption of light, this molecule is promoted to an excited state and is oxidized by the primary electron acceptor of Photosystem I, called X, which in turn is oxidized by the chain of electron carriers leading to the reduction of NADP. Upon absorption of light, P680 oxidizes Z, the intermediate which connects the photosystems to the water oxidizing apparatus. z^{+} is then reduced by electrons which originate from the oxidation of H₂O. Figure 2 shows the relative position of the electron chain components in the thylakoid membrane.

We will be concerned here with the water oxidation center located near the inner surface of the membrane. The charge separation steps which occur in this reaction center

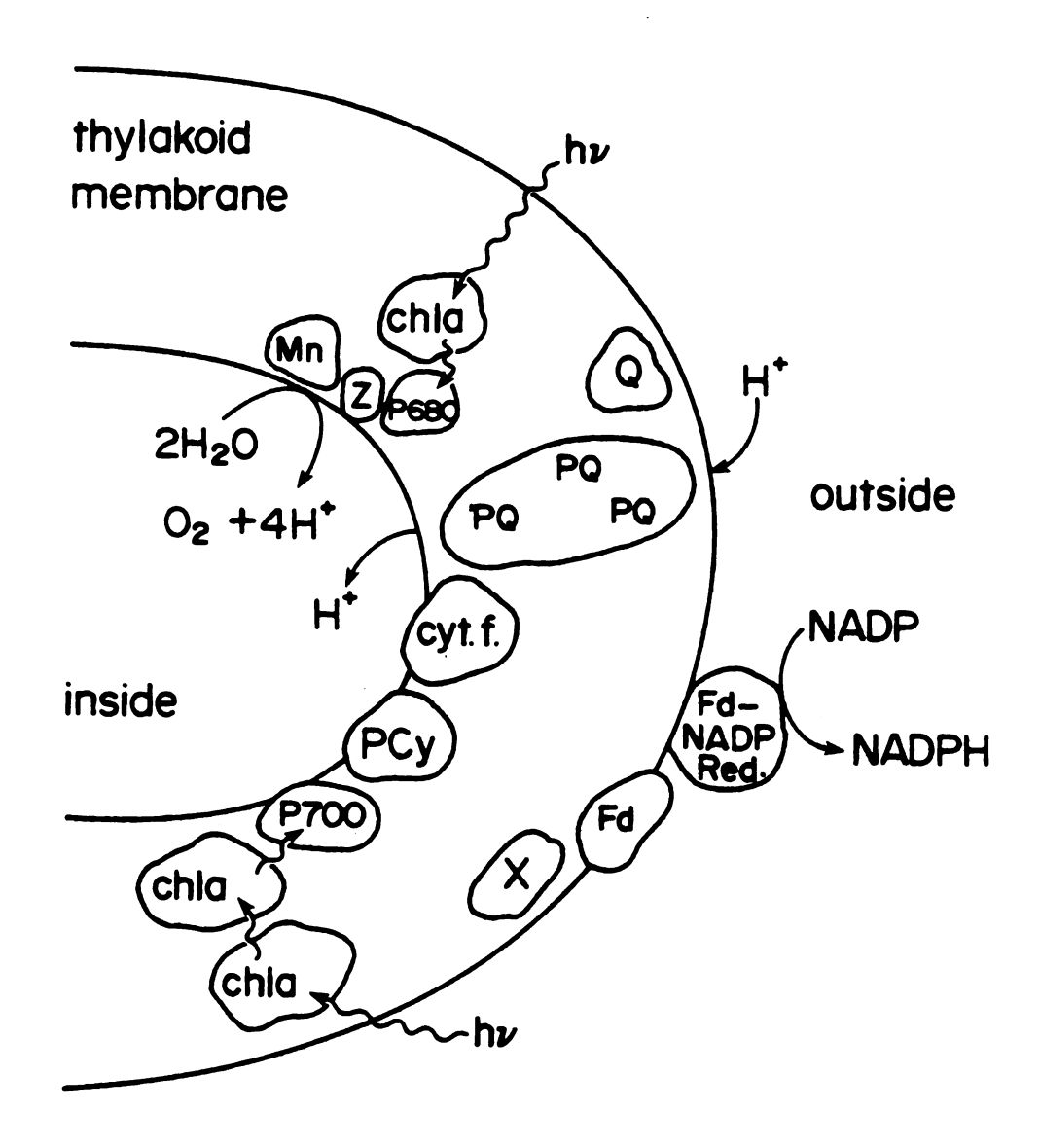


Figure 2. Schematic diagram of the thylakoid membrane showing the relative positions of the electron carriers described in Figure 1. Chl a represents antenae chlorophyll. Mn is the water oxidation complex. From [32].

are shown below:

$$ZP680Q \xrightarrow{hv} ZP680^{+}Q^{-}$$

$$ZP680^{+}Q^{-} \xrightarrow{2} Z^{+}P680Q^{-}$$

$$S_{n} + Z^{+}P680Q^{-} \xrightarrow{3} ZP680Q^{-} + S_{n+1}$$

$$A + ZP680Q^{-} \xrightarrow{4} ZP680Q + A^{-}$$

where A represents the electron carrier pool between the photosystems. Light induced charge separation occurs in the first step. In step two Z reduces P680 and in step three Z is reduced in turn by the water oxidizing system, S. The subscripts on S refer to the accumulation of oxidizing equivalents. Step four shows the reaction center returning to its original state by losing an electron to the next intermediate in the reducing side electron transport chain, A.

2. The S states

In 1969 Kok et al. and Joliot performed experiments aimed at an observation of the O₂ response pattern of chloroplasts exposed to a sequence of very short (20 µsec) actinic flashes of light, short enough to cause only one turnover of the light-activated system [3,4]. The results of one of these experiments, figure 3, show the relative amount of oxygen released from chloroplasts for each flash in the series. Very little oxygen is produced after

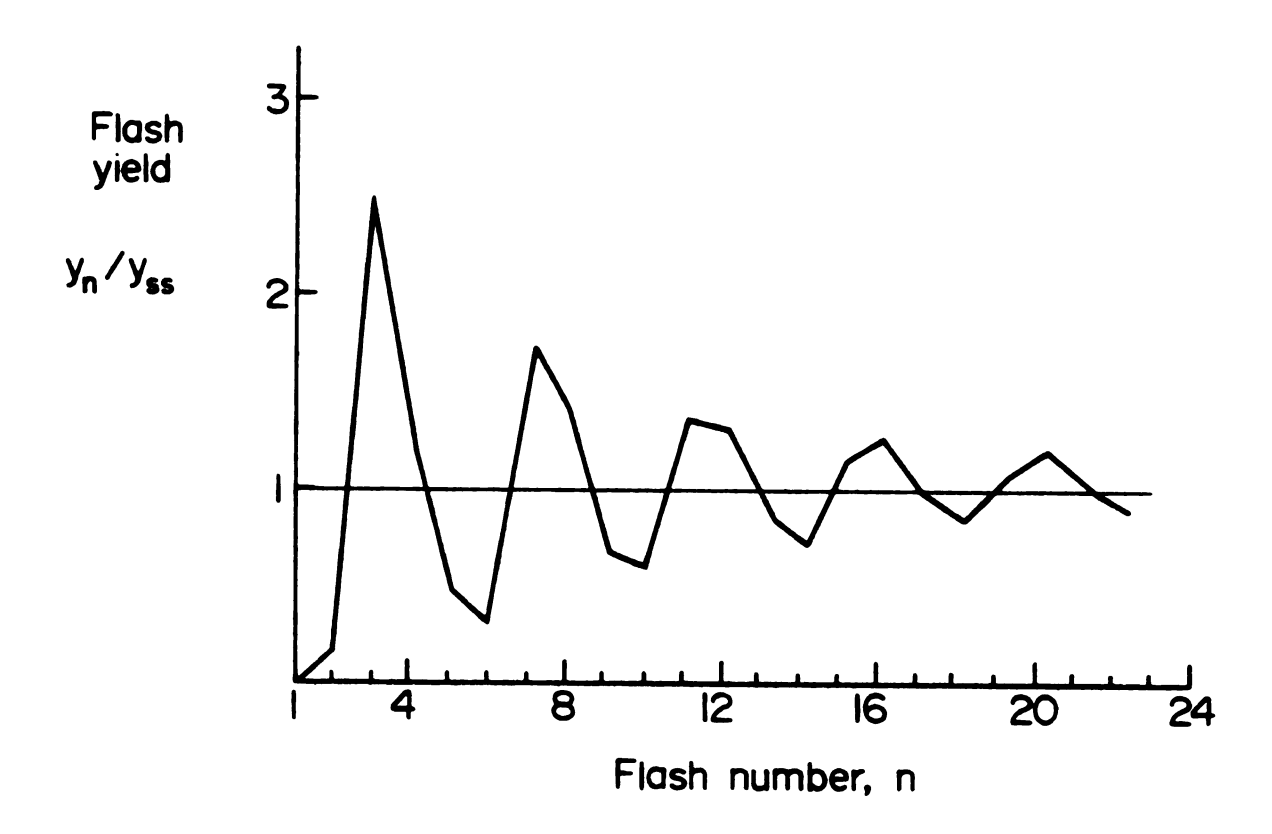


Figure 3. Ratio of amount of oxygen released from chloroplasts after a flash to the steady state yield of oxygen vs. flash number, n. From [3].

the first two flashes. After the third flash the amount of oxygen released is more than twice the steady state amount. After the next three flashes the amount of oxygen released is small but increases again after flash 7. The periodicity of four flashes shown by the oxygen release data led Kok to postulate the following model [3]:

$$s_0 \xrightarrow{h\nu} s_1 \xrightarrow{h\nu} s_2 \xrightarrow{h\nu} s_3 \xrightarrow{h\nu} s_4 \xrightarrow{2H_2O}$$

$$s_0 + O_2 + 4H^+ + 4e^-.$$

S represents the water oxidizing, oxygen producing system and the subscripts refer to the number of oxidizing equivalents stored in the system. Upon the absorption of four photons, the complex has enough energy to oxidize two H₂O molecules and release one O₂ and four electrons. Note that S represents that part of the photosynthetic process directly responsible for water oxidation and may represent more than one molecular species [38].

Kok's model has proven very useful although the original concept of its function as a charge accumulator which releases four protons concurrently with O₂ is not correct. More recent studies [5,34] have shown that protons are released in a stepwise fashion such as in the scheme below suggested by Fowler [5]:

$$S_{0} \xrightarrow{h\nu} S_{1} + H^{+}$$

$$S_{1} \xrightarrow{h\nu} S_{2}$$

$$S_{2} \xrightarrow{h\nu} S_{3} + H^{+}$$

$$S_{3} \xrightarrow{h\nu} S_{4} + 2H^{+}$$

$$S_{4} \xrightarrow{h\nu} S_{0} + O_{2} + 4e^{-}$$

This pattern indicates that the oxidation of two water molecules is not accomplished all at once but that each H₂O is bound by the S system separately so that each S state has a different configuration of water molecules around it. Several treatments which inhibit water oxidation (see below) have been found to attack the S₂ state, the formation of which as described above is not accompanied by proton release.

Chloride ion is essential to photosynthetic water oxidation [35-37]. Recently, Izawa and coworkers have found evidence which indicates that Cl is located in the S system at the site of inhibition of water oxidation by hydroxylamine and that its role is more than that of a counterion for proton release [35,36]. They suggest that Cl is a cofactor to an enzyme involved in water oxidation and is very closely associated with the manganese involved in this process.

3. Mn and oxygen evolution

Manganese has been considered essential to water

oxidation for some time. In 1966, Cheniae and Martin found that algae grown in a medium not containing manganese did not produce oxygen [6]. Within a half hour of addition of manganese to the growth medium, these same algae produced oxygen. Later, Cheniae and Martin determined that chloroplasts contain about six Mn per reaction center (400 chl) and that four of these six are necessary for oxygen evolution [7]. More recently Yocum et al. have found that oxygen evolving chloroplasts contain five Mn/400 chl of which four appear to be essential for oxygen evolution [8].

It is not clear how manganese functions in the water oxidation process. Soon after the appearance of Kok's S state model, the required presence of manganese for the system to function and the ability of the element to exist in higher oxidation states made it a candidate for a charge accumulator in the model. The proton release studies discussed above led some researchers to believe that this could not be so but others believe that one or more of the manganese involved changes oxidation state as the S states go through their cycle [31,39]. Evidence for this was presented in a recent article reporting EPR detection of a light induced change in manganese oxidation state [39] but the interpretation of the data in this article have been disputed [8].

It is quite possible that manganese remains in the +2 state and serves strictly as a structural coordinator in the membrane and/or as part of a protein. Direct evidence of this role for manganese has not been found due to the inability to probe the environment of manganese in functioning chloroplasts. However, the magnetic resonance studies offer indirect evidence for this role through detection of Mn(II) in nonfunctioning chloroplasts. The relaxation of protons by Mn(II) has been observed in NMR studies of chloroplasts in which oxygen evolution has been inhibited [9]. Hexaquo Mn(II) gives a characteristic EPR signal at room temperature and this signal is observed in chloroplasts treated to release manganese from its binding site [8]. These studies suggest that the manganese in the water oxidation complex remains in the +2 state, at least in inhibited, non-oxygen evolving chloroplasts.

4. Inhibitors of oxygen evolution

This section lists some treatments referred to in the research described below which inhibit oxygen evolution in chloroplasts. It is not a complete listing of known inhibitory treatments. Some others are heating, aging and treatment with chaotropic agents.

a) Ammonia

Velthuys and others before him have shown that NH₃ inhibits oxygen evolution in chloroplasts rapidly and reversibly [10]. Velthuys obtained inhibition by treating

chloroplasts with 50 mM $\mathrm{NH_4Cl}$ at pH 7.8. He found that that $\mathrm{NH_3}$ is able to attack the water oxidation complex in the $\mathrm{S_2}$ and $\mathrm{S_3}$ states and suggested that ammonia inhibits oxygen evolution by competing with water for binding sites in the water oxidation complex.

b) Hydroxylamine

It has been known for some time that hydroxylamine is an inhibitor of oxygen evolution [11], although the mechanism of inactivation is still not completely understood [12]. This is due at least in part to the fact that NH2OH serves as an electron donor to Photosystem II in chloroplasts unable to oxidize water [13]. Typical hydroxylamine concentrations used to inhibit oxygen evolution are in the 5 mM range. It has recently been found that the inhibition works best when the incubation is in the dark [12] and that the inhibition can be reversed by the addition of Mn²⁺ and light [14]. Treatment of chloroplasts with NH2OH does not release Mn²⁺ from the system [8,12].

c) Tris

Washing cloroplasts in 0.8 M Tris buffer (pH 8.0) is one of the most widely used treatments to inhibit water oxidation. The treatment works best in the light and is reversible by washing with reducing agents [18]. Cheniae and Martin have found that, like NH $_3$, Tris inhibits water oxidation by attacking the S $_2$ state [15]. Treatment of chloroplasts with Tris releases one Mn $^{2+}$ from the reaction

center [8]. Electron flow through Photosystem II can be restored, without reactivating O_2 evolution, by providing the inhibited chloroplasts with an electron donor and light. This observation provides strong evidence that the action of Tris is specific to the water oxidizing center. d) Ca^{2+}

In describing the above inhibitory treatments it has been pointed out that ammonia and hydroxylamine do not cause release of Mn²⁺ from its site in the membrane and that Tris releases one Mn/400 chl. Previous reports describing these treatments indicated the amount of manganese released is greater but recent reports show that these earlier studies were done with chloroplasts containing nonfunctional Mn²⁺, i.e., Mn²⁺ not essential to the water oxidation process [8,9,16]. This nonfunctional Mn²⁺ can be removed by grinding the original leaves in the presence of 1 mM EDTA [9,17].

 ${\rm Ca}^{2+}$ does not inhibit oxygen evolution. However, addition of 50 mM ${\rm CaCl}_2$ to ${\rm NH}_2{\rm OH}-$ or Tris-treated chloroplasts prepared in the presence of 1 mM EDTA results in an increase in the amount of ${\rm Mn}^{2+}$ released from the membrane as observed by EPR [8]. It is thought that ${\rm Ca}^{2+}$ is able to displace ${\rm Mn}^{2+}$ which has been perturbed in its binding site by the inhibitory treatment. This effect is not peculiar to ${\rm Ca}^{2+}$ as ${\rm Zn}^{2+}$ (but not ${\rm Mg}^{2+}$) has also been found to displace ${\rm Mn}^{2+}$ in inhibited chloroplasts.

B. Mn²⁺ EPR SIGNAL

The nature of the aqueous Mn²⁺ ion makes it easily detectable by EPR at room temperature. Since most of the experiments reported in this thesis are dependent on the detection of the EPR signal due to Mn²⁺ ions in chloroplasts samples, a brief explanation of the origin of this signal will aid in the understanding of the reported results. The treatment here follows those of Blankenship and Wertz and Bolton [18,19].

The Mn^{2+} ion has the electronic configuration (Ar)3d⁵. It is a high spin ion (S = 5/2) and so is in the ⁶S spectroscopic state. That is, the five d electrons are oriented with their spin parallel and have zero net orbital angular momentum (L = 0). For systems with L \neq 0, electronic transitions are made possible through relaxation by lattice vibrations through spin-orbit coupling. To observe the EPR spectrum, these lattice vibrations must be quenched by lowering the temperature. In the Mn^{2+} system the orbital angular momentum is zero and there is no spin-orbit coupling. The excited electronic states are at too high an energy for transitions to occur. Since there is no need to quench any lattice vibrations the EPR spectrum is seen at room temperature.

The spin Hamiltonian for a paramagnetic free ion with no crystal field present or in an isotropic field is given by equation (2):

$$H = g\beta H\hat{S} - g_N \beta_N H\hat{I} + a\hat{I} \cdot \hat{S} . \qquad (2)$$

Here g is the Lande' g factor; β is the Bohr magneton; g_N and β_N are their nuclear counterparts; H is the magnetic field; \hat{S} is the electron spin; \hat{I} is the nuclear spin; and a is the hyperfine splitting constant. The first term is the electron Zeeman interaction and is the most important. The second term is the nuclear Zeeman interaction. It is very small and is ignored here. The third term is the hyperfine interaction between the electronic and nuclear spins.

From the Zeeman term we obtain the following eigenvalues:

$$E_{5/2} = 5/2g\beta H$$
 $E_{-1/2} = -1/2g\beta H$ $E_{3/2} = 3/2g\beta H$ $E_{-3/2} = -3/2g\beta H$ $E_{-1/2} = -5/2g\beta H$

According to the selection rule, $\Delta M_S = 1$, there are five possible transitions, all with the same energy, $E = g\beta H$. If the Zeeman term were the only term in Eq. (2), then transitions would occur as shown in figure $\underline{4}$, resulting in the observation of a single line.

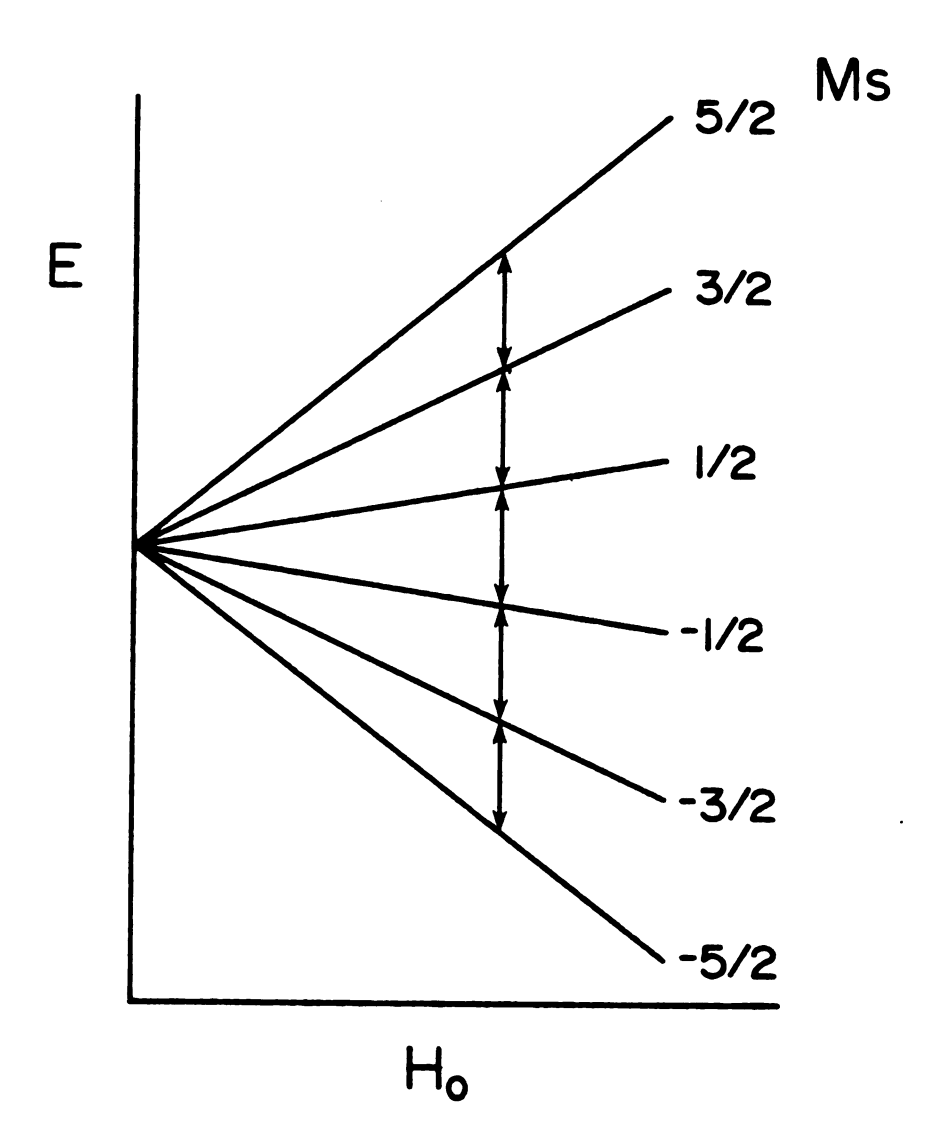


Figure 4. Diagram showing the degeneracy of the five $\rm M_{\rm S}$ transitions of the $\rm Mn^{2+}$ ion with no crystal field present. From [18].

The nuclear spin of 55 Mn (100% abundance) is I = 5/2 and this makes the hyperfine interaction, $\hat{al\cdot S}$, very important. The nuclear spin splits each of the M_S states into six (2I = 1) separate energy levels. According to the selection rule, $\Delta M_I = 0$, each of the degenerate M_S transitions splits into six equal intensity lines. As an example, the hyperfine splitting of the $\frac{1}{2}$ \longleftrightarrow $-\frac{1}{2}$ transition is shown in figure $\frac{5}{2}$. Thus the EPR spectrum of Mn²⁺ in the absence of a crystal field will be a six line spectrum. See figure $\frac{6}{2}$.

If the Mn^{2+} ion is in an unsymmetric octahedral field, we must add to the spin Hamiltonian terms including the zero field splitting parameters, D and E, so that the spin Hamiltonian is now given by equation (3):

$$H = g\beta H\hat{S} - g_N^{\beta} \beta_N H\hat{I} + a\hat{I} \cdot S + D(\hat{S}_z^2 - 1/3\hat{S}(\hat{S} + 1)) + E(S_x^2 - S_y^2) .$$
(3)

The D term describes the amount of distortion along the Z-axis while the E term describes the distortion in the X-Y plane. For the aqueous ion, rapid tumbling in solution averages these distortions to zero and the D and E terms are not important. However, if the ion is in a more complex environment, for instance, bound to a protein or membrane, these parameters will broaden the signal described earlier (figure 6).

The linewidth broadening due to the contributions of the D and E parameters in complex environments is related to an increasing correlation time for molecular

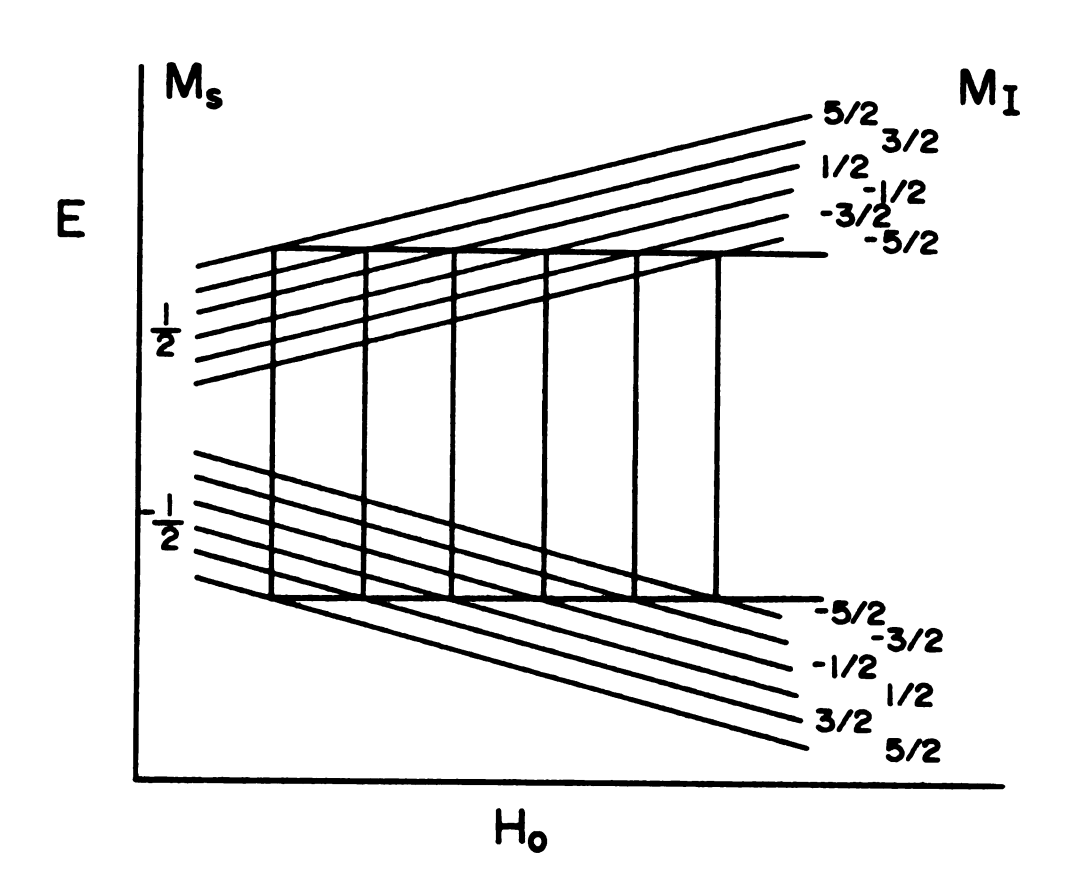


Figure 5. Diagram showing the six $M_{\bar{1}}$ transitions for the $\frac{1}{2} \longleftrightarrow -\frac{1}{2} M_{S}$ transition in the Mn²⁺ ion. From [18].

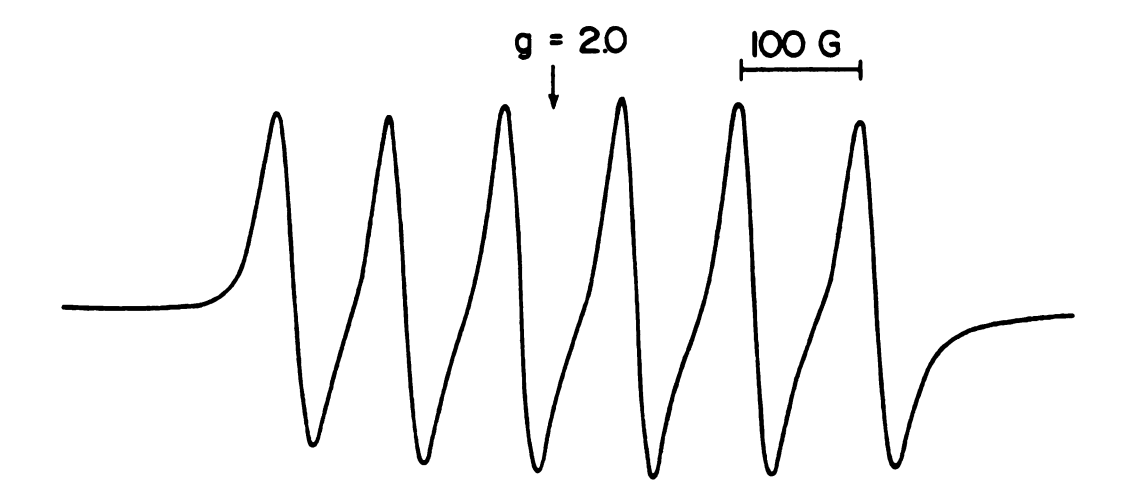


Figure 6. Room temperature solution ESR spectrum of $\mathrm{Mn^{+2}\,(H_{2}O)_{\,6}}.$ From [18].

rotation. As the rotation of the ion is slowed by more complex and tightly binding ligands, local anisotropies become more important and the linewidth increases. This relation between the linewidth, Γ , and the correlation time, $\tau_{\rm C}$, is seen in this general and simplified equation [19]:

$$\Gamma = \Gamma_0 + k\tau_C$$

where Γ_0 is the linewidth of the free ion (small τ_c) and k is a constant. As rotational motion slows and τ_c gets larger, the linewidth increases.

Reed, Leight and Pearson have shown that as $\tau_{\rm C}$ increases with the complexity of the liganding species, the signal is broadened [28]. For instance, the $\tau_{\rm C}$ for the hexaquo ion is 3.3 × 10⁻¹² sec while $\tau_{\rm C}$ for the EDTA complex, the signal of which is so broad as to not be observed, is 8.4 × 10⁻¹² sec.

If the manganese in the water oxidation complex is in the +2 state, its EPR spectrum will be broadened due to the large correlation time expected for an enzyme or membrane-bound system. In addition to this, there are at least four manganese atoms involved in the water oxidizing complex and it has been found that high concentrations of Mn²⁺ ions (close proximity of the ions) leads to interionic relaxation effects and a broadened spectrum [30]. In this model, the Mn²⁺ EPR signal is not observed until the manganese is displaced from its binding site.

This discussion has dealt with the EPR signal of the Mn²⁺ ion and may have given the impression that the manganese involved in water oxidation remains always in the +2 state. This is entirely possible. It is also quite possible that the manganese involved changes oxidation state with the S-states and that treatments which inhibit water oxidation arrest the oxidation state of the manganese at +2, leading to observation of the EPR signal upon its release from the membrane. Recently, a paper has been published which reports the observation of an EPR signal in intact chloroplasts at low temperature (25°K). Based on model systems, the 21 line signal is proposed to be due to a mixed valence complex of two or four manganese atoms [31].

C. AN INVESTIGATION INTO THE EFFECTS OF CHOLIC ACID AND AMMONIUM SULFATE ON MANGANESE IN THE WATER OXIDATION COMPLEX OF CHLOROPLASTS

1. Introduction

The possibility that the Mn which is required for oxygen evolution in photosynthesis is bound to some protein has led to several attempts to isolate a Mn-containing protein, the presence of which is necessary for water oxidation to occur in chloroplasts. Spector and Winget reported a successful attempt [20]. Their isolation procedure involved incubating chloroplasts in a mixture that was 0.4 M in $(NH_4)_2SO_4$ (pH 8.0); 50 mM in cholic acid; 0.1 M Sucrose; 0.01 M Tricine (pH 8.0); 1.5 mM MgCl₂. Chlorophyll concentration was 2 mg/ml. The mixture was stirred on ice for fifteen minutes. After ultracentrifugation the Mn protein was reported to be in the supernatant and the membranes in the pellet could not produce oxygen from water. Treatment of the supernatant with decreasing concentrations of (NH₄)₂SO₄ followed by filtration through Sephadex gels led to the isolation of a colorless 65 KD protein. When this protein was sonicated into liposomes containing the chloroplast membranes from the ultracentrifuge pellet, oxygen evolution was observed.

We have tried to repeat this procedure but have been unable to produce the desired results. We interpret our failure to reproduce the results of Spector and Winget as indicating that the 65 KD protein does not contain manganese and may not be essential for water oxidation.

Results supporting these conclusions are presented in this section which describes experiments performed on the pellet and the supernatant obtained by ultracentrifugation of the chloroplast suspension treated with cholic acid and ammonium sulfate.

2. Methods

a) Spinach Preparation

All chloroplast samples used in this study were prepared from market spinach. The washed, dark adapted spinach leaves were ground in a Waring blender in a medium that was 0.4 M Sucrose, 0.04 M Hepes, (pH 8.0), 0.4 M NaCl, 6 mM MgCl₂ and 1 mM EDTA. The suspension was centrifuged for six minutes at 6000 RPM and the supernatant discarded. The pellet was resuspended in a medium containing 0.4 M Sucrose, 0.04 M Hepes (pH 8.0) and 6 mM MgCl₂. The suspension was centrifuged, the supernatant discarded, and the pellet resuspended. This washing procedure was performed twice to remove EDTA left from the grinding step. Chlorophyll concentration of the final suspension was determined by the method of Sun and Sauer [21]. The cholic acid extraction was carried out as described by Spector and Winget [20]. Hydroxylamine,

Tris and HCl treatments were carried out by combining chloroplasts suspension, cholate-ammonium sulfate pellet suspension or cholate-ammonium sulfate supernatant with the appropriate reagent in a 1:1 by volume ratio to give the desired reagent concentration. Hydroxylamine incubation was carried out on ice in the dark for twenty minutes; Tris incubation was carried out on ice in room light for twenty minutes.

EDTA was included in the grinding step to remove loosely bound Mn²⁺ which is not part of the water oxidation apparatus. Recent studies have shown that failure to include this reagent in chloroplast preparation leads to high and misleading values of Mn²⁺ content in EPR studies [8].

Spector and Winget reported using Tricine as the buffer in their chloroplast suspension. Here, Hepes buffer was used in place of Tricine because Tricine is a chelator of Mn^{2+} . Figure $\underline{7}$ shows the effect of increasing concentration of Tricine and Hepes on the EPR signal of 100 μM MnCl₂.

b) EPR Measurements

EPR spectra were obtained at room temperature by using a Varian E-4 spectrometer. The cavity was continuously flushed with dry nitrogen. Instrument settings are noted in the figure captions.

All samples were contained in a Scanlon quartz TE mode cavity flat cell, model S-812. The flat cell was

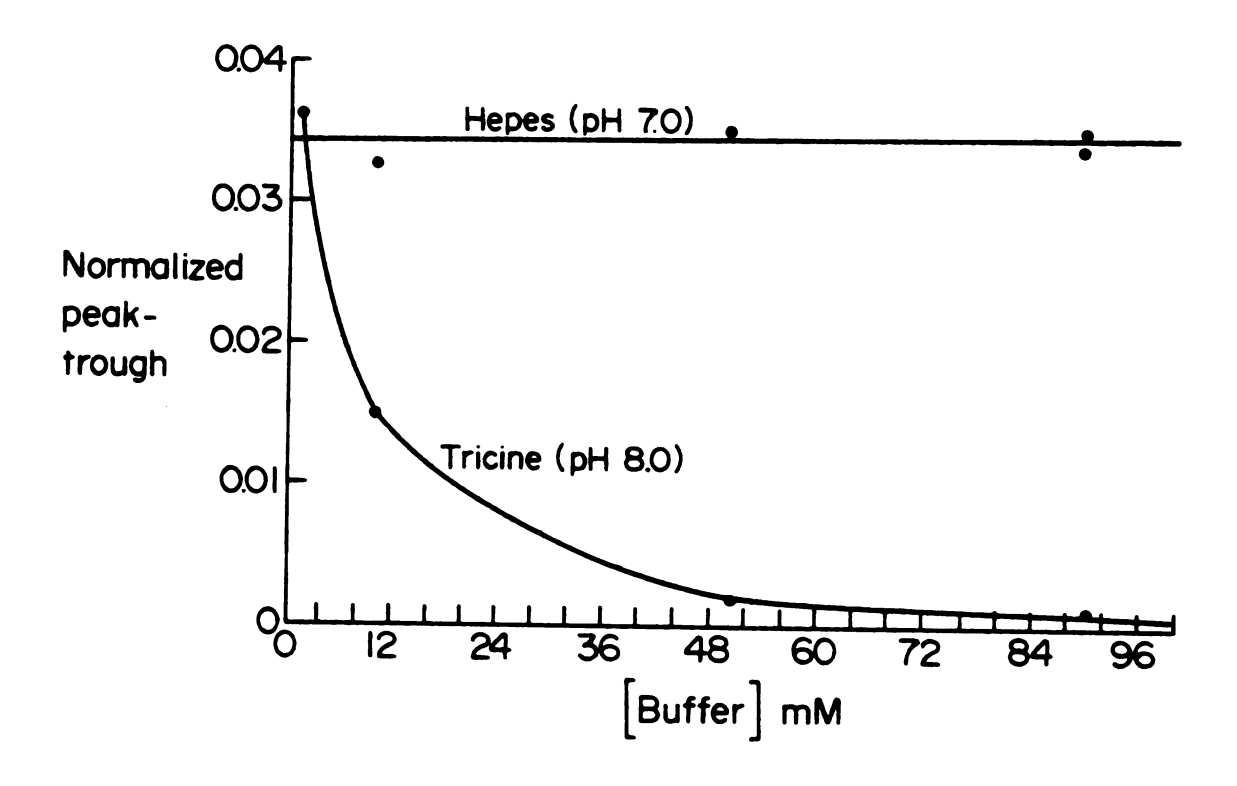


Figure 7. Normalized peak to trough distance of the third line of the EPR spectrum of 100 μM MnCl $_2$ vs. Tricine (pH 8.0) and Hepes (pH 7.0) concentration.

marked so that sample positioning could be reproduced as closely as possible. Illumination of samples in the cavity was done using a Bausch and Lomb microscope lamp, model 313539.

Concentration of Mn²⁺ in a sample was determined by using the calibration curve shown in figure 8. The calibration curve plots normalized peak to trough amplitude of the third line from the left of the Mn²⁺ spectrum against concentration of MnCl₂ at pH = 8.0. Normalized peak to trough amplitude was determined by dividing the measured peak to trough amplitude in centimeters by the instrument gain setting. It was found that the free base present in 0.8 M Tris (pH 8.0) and in 0.4 M (NH₄)₂SO₄ (pH 8.0) complexes Mn²⁺ so as to make some of the Mn²⁺ present undetectable by EPR, thus lowering the calibration curve. The reported amounts of Mn²⁺ released in Tables 1 and 2 have been corrected for the effects of these reagents.

c) Oxygen measurements

Oxygen evolution was measured by using an oxygen electrode, model YSI 5331, Yellow Springs Instrument Co. The electrode consists of a platinum cathode and a silver anode in a KCl solution kept over the electrode by a Teflon membrane. When a polarizing voltage is applied across the electrode, (typically -0.6 volts vs. a silver/silver chloride reference electrode), oxygen is reduced at the cathode:

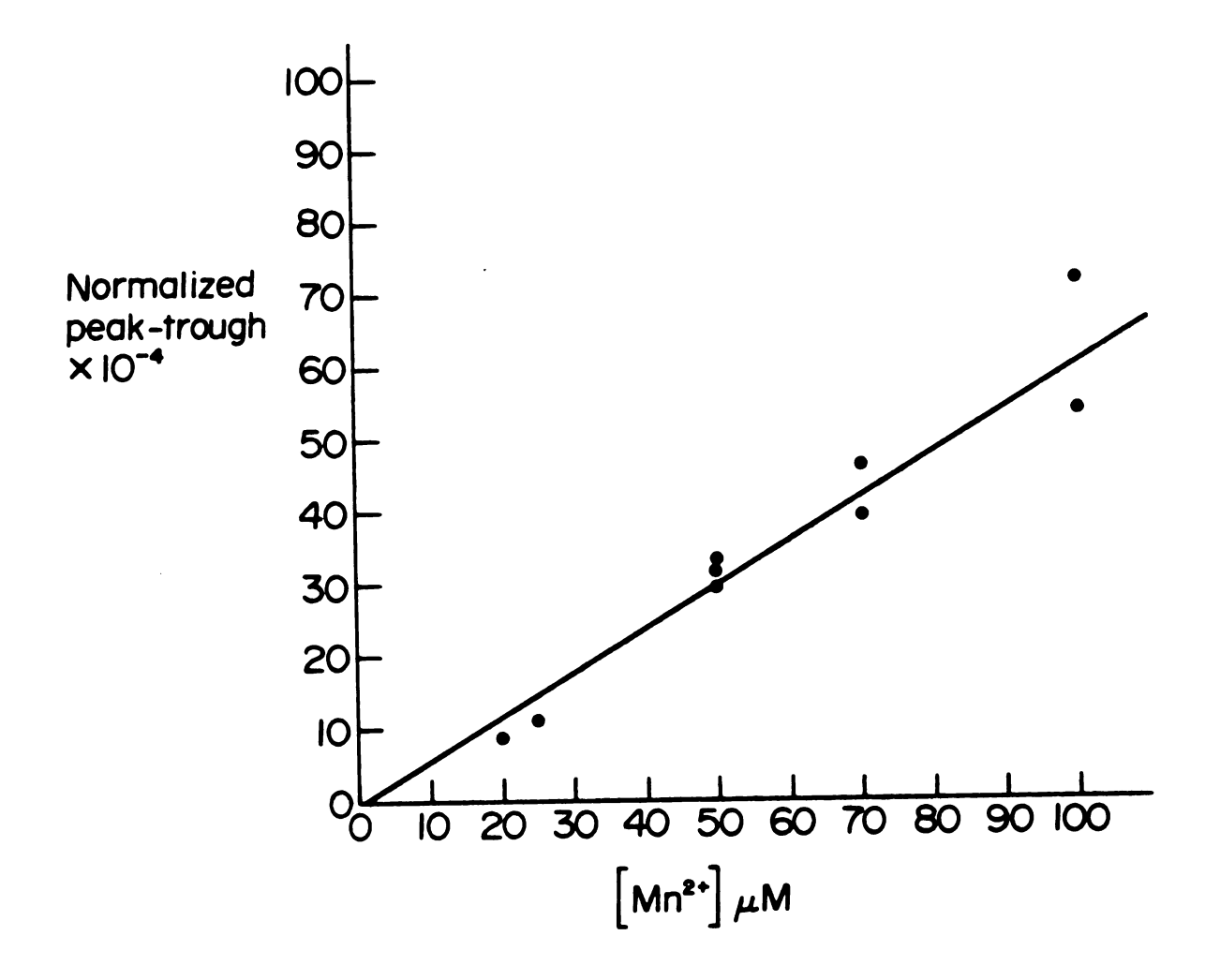


Figure 8. Calibration curve for determination of $\rm Mn^{2+}$ concentration in Hepes buffer (pH 8.0) from normalized peak to trough distance of the third line of the EPR spectrum. Slope of the line is 0.67 cm \times 10^{-4} (normalized)/ μ M Mn²⁺ at 10 G modulation amplitude, 100 mW.

$$O_2 + 2H_2O + 4e^- \longrightarrow 4OH^-$$
.

The anode reaction is:

$$4Ag + 4Cl \longrightarrow 4AgCl + 4e$$
.

Oxygen diffuses across the membrane at a rate proportional to its concentration [32]. To keep the oxygen concentration in the sample chamber uniform, the sample is constantly stirred by a magnet stir bar. The tip of the electrode lies flush with the side of the sample chamber (6 cm high; radius of 0.75 cm) which is housed in a lucite cube (7.5 cm high) through which is flowed temperature controlled water from a Forma Scientific model 2095 bath circulator. The surface of the electrode tip is parallel to the light path.

White light from a General Electric 200 W projector lamp is passed through a heat absorbing filter and a set of neutral density filters and is focused on the sample chamber by a pair of planoconvex lenses. Figure 9 shows a light saturation curve indicating the light intensity was sufficient for optimal results.

Current detection from the electrode was accomplished with a Yellow Springs Instrument Co. Oxygen Monitor, model 53 (donated by Dr. C.F. Yocum) attached to a Heath Strip Chart recorder, model SR255B or with the detection system described by Yerkes [32]. The system was calibrated by bubbling water with nitrogen ($[O_2] = 0$), air ($[O_2] = 240~\mu\text{M}$) and oxygen ($[O_2] = 1.14~\text{mM}$). The reaction solution for

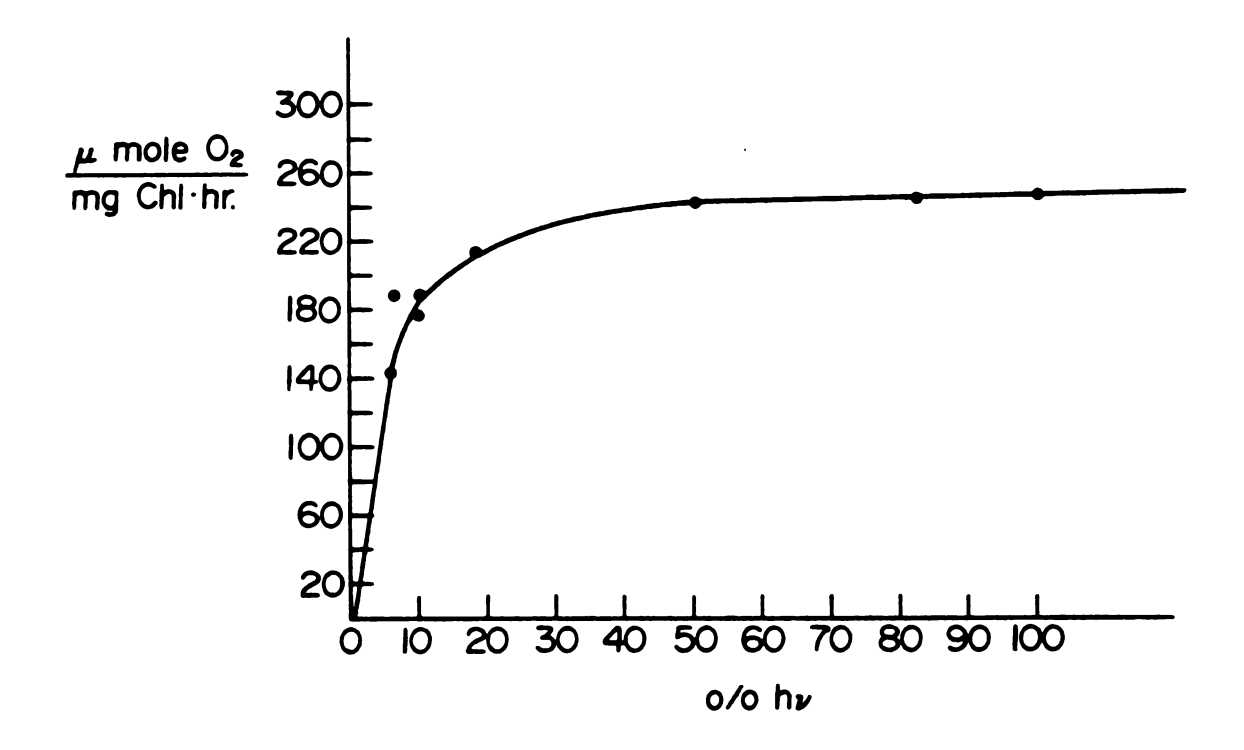


Figure 9. Light saturation curve for chlorophyll at 10 μ g/ml in the oxygen electrode system described in the text. Light intensity controlled with neutral density filters.

oxygen evolution contained 50 mM Hepes, 20 mM NaCl, 10 mM NH₄Cl, 5 mM MgCl₂ and 1 mM NaCN at pH = 7.6. The electron acceptor was 0.5 mM methyl viologen. When necessary, 0.5 mM diphenyl carbazide was used as exogenous electron donor. The diphenyl carbazide was dissolved in 95% EtOH at a concentration of 0.08 M. The resulting concentration of EtOH present in the oxygen electrode chamber was 0.48%.

The use of methyl viologen as electron acceptor results in the observation of recorded oxygen uptake rather than oxygen evolution from illuminated chloroplasts because of the following reactions:

$$2H_{2}O \xrightarrow{\text{light}} O_{2} + 4H^{+} + 4e^{-}$$

$$4H^{+} + 4e^{-} + 2MV_{OX} \xrightarrow{} 2MV_{red}$$

$$2MV_{red} + 2O_{2} \xrightarrow{} 2MV_{OX} + 2H_{2}O_{2}$$
overall:
$$2H_{2}O + O_{2} \xrightarrow{} + 2H_{2}O_{2}$$
 (4)

i.e., the reduction of methyl viologen causes a depletion in oxygen owing to the formation of H_2O_2 . NaCN is added to the reaction mixture to stop the action of peroxidase shown in the following reaction:

$$2H_2O_2 \xrightarrow{\text{peroxidase}} 2H_2O + O_2$$
 (5)

If this reaction were not inhibited by the added NaCN, reactions (4) and (5) would add up to no net change and

we would not observe the oxygen uptake indicated in reaction (4).

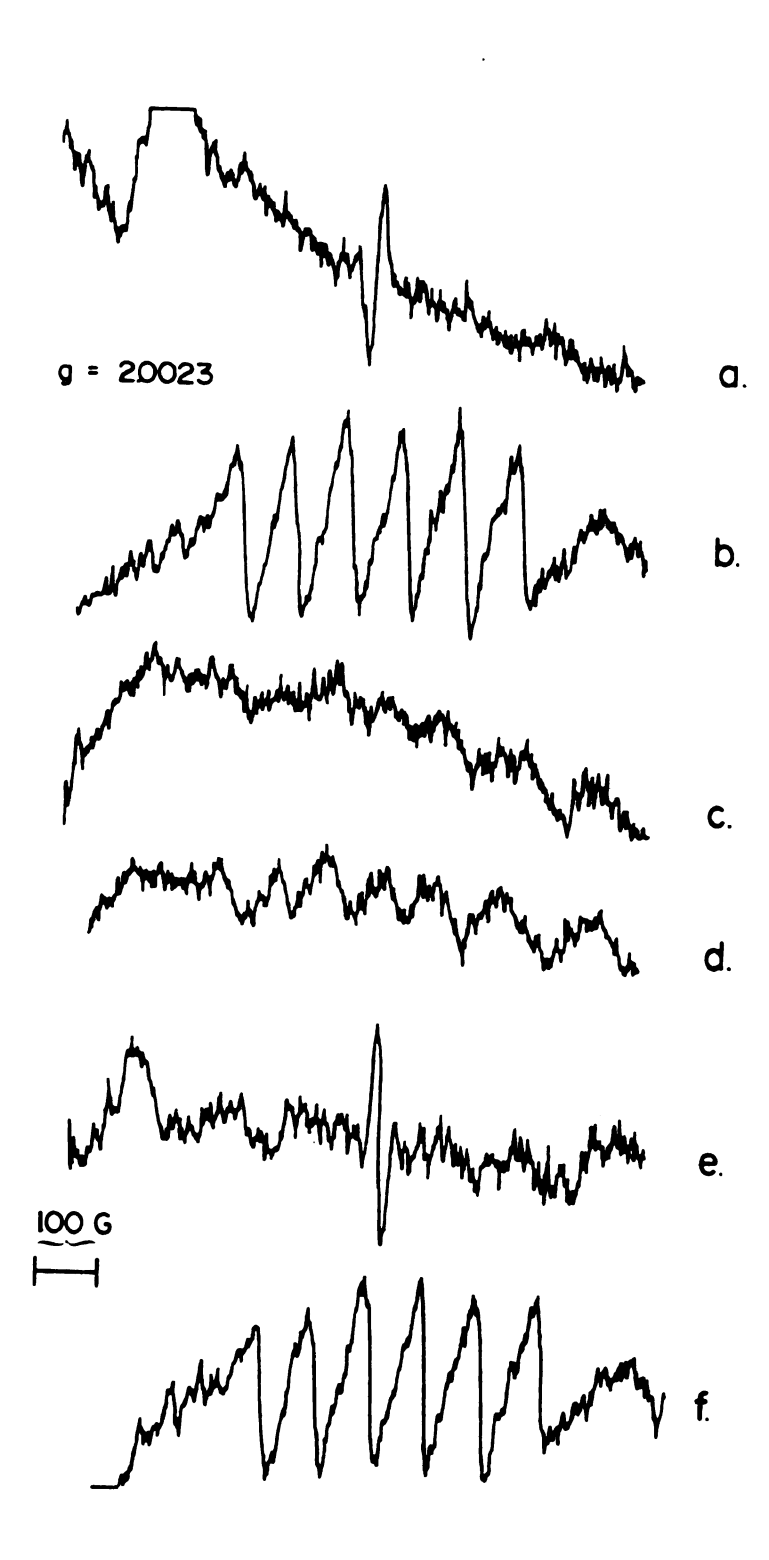
3. Results

- Mn²⁺ Content in Cholate Pellet and Cholate Supernatant Treatment with 1 N HCl is known to release all Mn 2+ from chloroplast membranes and to denature all proteins. Figure 10 shows the EPR spectra of chloroplast suspension, cholate supernatant and cholate pellet before and after treatment with 1 N HCl. The concentration of Mn²⁺ corresponding to these signals and the total amount of manganese present in the chloroplasts, pellet and supernatant as determined by using EPR are given in Table 1. The total number of Mn²⁺ per reaction center in untreated chloroplasts is 5 Mn²⁺/400 chl (the ratio of chlorophyll to reaction center is 400/1). Of this total, $4 \text{ Mn}^{2+}/400$ chl remain in the membrane after extraction with cholic acid and ammonium sulfate. Of the Mn²⁺ which is found in the supernatant, nearly half of it is EPR-detectable before acidification indicating that this portion of the Mn²⁺ released is not bound to a protein. These data indicate that treatment with cholic acid and ammonium sulfate removes one manganese per reaction center and only about half this amount is bound.
- b) Effect of NH₂OH and Tris on the Cholate Pellet

 As described in the introduction, treatment with NH₂OH

 or Tris buffer inhibits oxygen evolution in chloroplasts.

Figure 10. EPR spectra of (a) chloroplast suspension; (b) chloroplast suspension in 1 N HCl; (c) supernatant from cholic acid treatment; (d) supernatant from cholic acid treatment in 1 N HCl; (e) pellet from cholic acid treatment; (f) pellet from cholic acid treatment in 1N HCl. Instrument settings for all spectra are: Field width, 1000 G; Modulation amplitude, 10 G; Time constant, 0.3 sec.; Scan time 4 min.; Power, 100 mW; Frequency, 9.45 GHz; Gain, 2 × 10⁴.



- Manganese Released by Various Treatments from Chloroplasts, Cholate Pellet and Cholate Supernatant as Detected by Using EPR. TABLE 1

| Sample | Treatment | [Mn ²⁺]* | Mn/400 Chl Released* | Total Mn in Sample** (nmoles) |
|--------------|--|-------------------------------|--|-------------------------------|
| Chloroplasts | none lN HCl | | 5.10 | 1146 |
| Pellet | none 1N HC1 50 mM CaCl ₂ 5 mM NH ₂ OH 5 mM NH ₂ OH and 50 mM CaCl ₂ 0.8 M Tris (pH 8.0) 0.8 M Tris and 50 mM CaCl ₂ none 1N HCl 50 mM CaCl ₂ 0.8 M Tris (pH 8.0) 0.8 M Tris (pH 8.0) | 5.02 11.15 5.14 5.64 | 1.19 4.05 2.18 1.64 3.23 2.55 2.30 | 397 |
| | 50 mm caci2 | 5.91 | | |

400 chl = one reaction center. These data are the average of measurements made on samples prepared from chloroplasts with chlorophyll concentrations ranging from 2.8 mg/ml *Detected by EPR. 3.5 mg/ml. **[Mn²⁺] detected by EPR. Total Mn calculated by multiplying [Mn²⁺] times the volume of the sample. These data are the average of measurements made on samples prepared from chloroplasts with chlorophyll concentration of 3.04 mg/ml. In chloroplasts both treatments affect the manganese ion or its environment in a way which makes the ${\rm Mn}^{2+}$ easily displaced by high concentrations of ${\rm Ca}^{2+}$.

Figure $\underline{11}$ shows the effect of increasing hydroxylamine concentration of Mn^{2+} release from the cholate pellet and listed in Table 1 are the amounts of Mn^{2+} released from the pellet by $\mathrm{NH_2OH}$, Tris , Ca^{2+} , $\mathrm{NH_2OH}$ and Ca^{2+} , and Tris and Ca^{2+} as measured by EPR. Note that it was pointed out in the introduction that $\mathrm{NH_2OH}$ does not release Mn^{2+} from chloroplasts. The Mn^{2+} released by $\mathrm{NH_2OH}$ reported here is from chloroplasts which have gone through the cholic acid/ammonium sulfate treatment.

We see from this data that of the four manganese atoms per reaction center left in the pellet after cholic acid treatment one is released from its binding site. Another is loose enough in its binding site that addition of Ca²⁺ can release it. Hydroxylamine attacks at least one other manganese as indicated by the observation of three manganese per reaction center in the presence of NH₂OH plus Ca²⁺, two more than observed in the untreated pellet and one more than observed in the presence of Ca²⁺ only. Also note in Figure 11 that the number of manganese released per reaction center in the pellet by increasing NH₂OH concentration reaches a limit just under three. Treatment with Tris releases one more manganese than found in the untreated pellet but addition of Ca²⁺ with

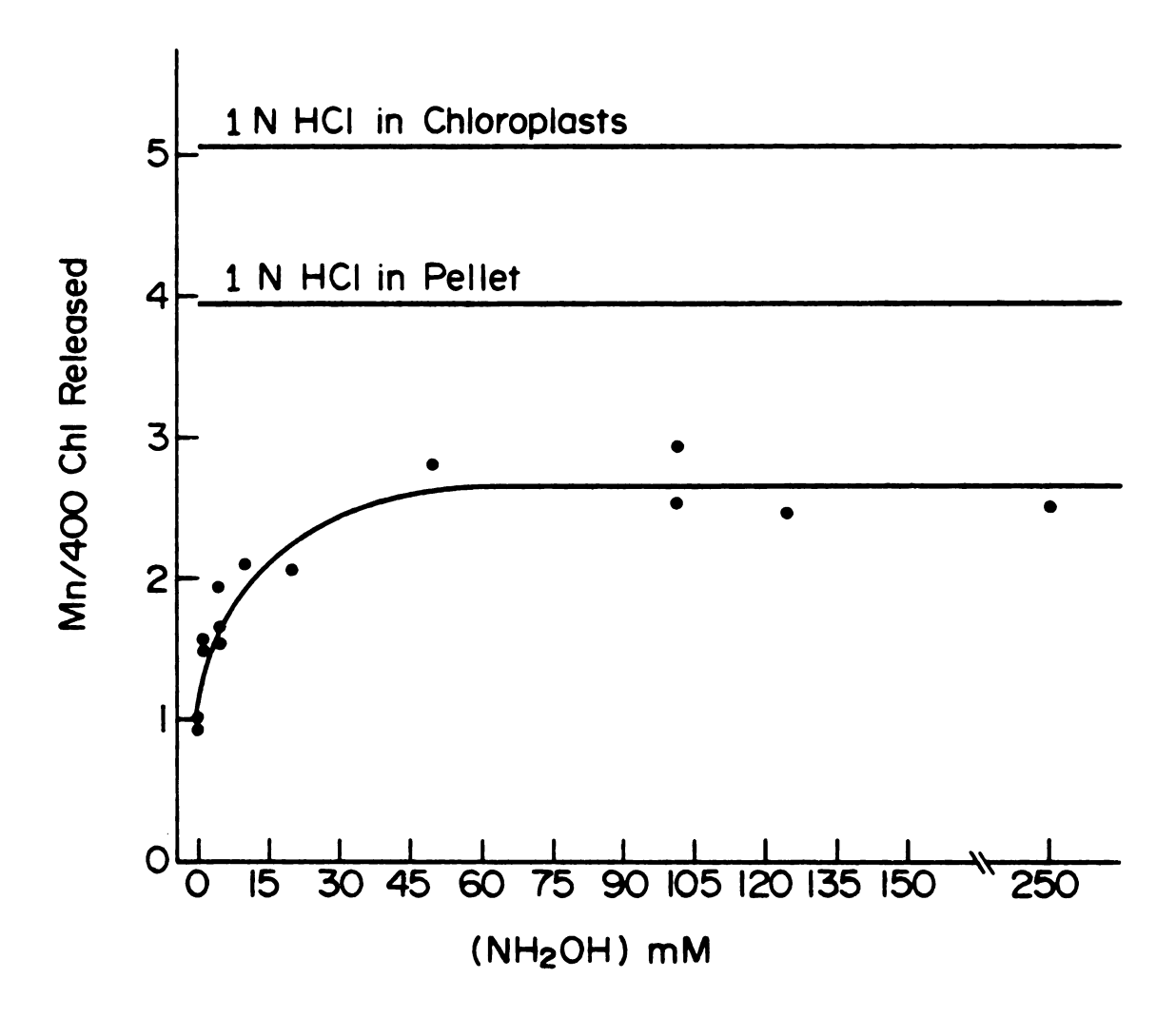


Figure 11. Graph showing the amount of Mn^{2^+} released from the cholate pellet by increasing concentration of hydroxy-lamine as detected by EPR. Also shown are the amounts of Mn^{2^+} released from the pellet and from untreated chloroplasts by 1 N HCl.

indicating either that the manganese released by Tris is the same as that released by ${\rm Ca}^{2+}$ or that Tris releases one manganese and protects the one released by ${\rm Ca}^{2+}$.

The inhibition of water oxidation by Tris and by hydroxylamine appears to occur by different mechanisms. Tris inhibition works best in the light while inhibition by NH2OH works best in the dark. Frasch and Cheniae have found that Tris inactivates by complexing the S2 state. Inactivation of a chloroplast sample containing 50 μg chl/ml requires an unprotonated Tris concentration of about 500 mM [42]. The concentration of unprotonated Tris depends both on Tris concentration and on pH. Hydroxylamine inactivation of water oxidation in chloroplast samples containing 300 µg chl/ml is achieved with a concentration of NH2OH of 5 mM at pH 8.0 [12]. Recent evidence indicates that these treatments affect the manganese in the oxygen evolving center differently [8]. NH2OH attacks three manganese which can only be released by addition of Ca²⁺. Tris attacks two manganese, one of which is released outright and the other requiring Ca2+ addition for release.

Table 1 also shows that treatment of the supernatant with Tris, Ca^{2+} or Tris plus Ca^{2+} releases only a small amount of bound manganese.

c) Individual Effects of Cholic Acid and Ammonium Sulfate on Chloroplasts

Ammonia inhibits oxygen evolution in chloroplasts by a process which can be reversed by subsequent buffer wash

steps [10]. To determine whether the inhibition of oxygen evolution observed following cholate extraction was caused by the introduction of NH_3 in the form of $(NH_4)_2SO_4$, the pellet which resulted from the cholate/ammonium sulfate extraction was washed in the suspension medium (see p. 9) several times in order to remove residual ammonium sulfate and assayed for oxygen evolution. The washed membranes from the cholate pellet could not evolve oxygen from water (data not shown).

To observe the individual effects of cholic acid and ammonium sulfate on chloroplasts, a sample of chloroplasts was divided into three parts and treated as in the cholate extraction with the following modifications:

(A) cholic acid was excluded; (B) ammonium sulfate was excluded; (C) no exclusions. Chloroplasts in preparation (A) were exposed to ammounium sulfate, those in (B) were exposed only to cholic acid and (C) was the control. The samples were not centrifuged. The treated chloroplasts were assayed for oxygen evolution in the oxygen electrode and for Mn²⁺ release by EPR. Table 2 lists the amount of Mn²⁺ released as detected by EPR in each sample and their rates of oxygen evolution.

The data in Table 2 indicate that treatment of chloroplasts with 0.4 M $(\mathrm{NH_4})_2\mathrm{SO_4}$ (pH 8.0) results in the release of about 1.5 manganese per reaction center and this amount is not increased by the addition of Ca^{2+} . Cholic

TABLE 2 - Individual Effects of Cholic Acid and Ammonium Sulfate on Manganese Release and Oxygen Evolution in Chloroplasts.

| Released* Electron Transfer Rates** (electron donor) | H ₂ O DPC moles O ₂ mg chl·hr | 0 168 | 3 0 52 | | 0 91 | | 340 |
|--|---|--------------------------------|--------|---|------|-----------------------------------|----------------|
| Preparation Mn/400 Chl Released* | | A (ammonium sulfate only) 1.45 | 14) | B in 50 mM CaCl_2 1.60 | | c in 50 mM CaCl ₂ 1.76 | Chloroplasts 0 |

*Detected by EPR. Chloroplast samples used contained 4.0 mg chl/ml.

^{**}Measured by oxygen uptake.

acid attacks one to two binding sites but release of the manganese requires the presence of Ca²⁺. When chloroplasts are treated with both ammonium sulfate and cholic acid, the effect of ammonium sulfate appears to be stronger as no increase in Mn²⁺ is observed upon the addition of Ca²⁺. This indicates that the NH₃ present as free base in the ammonium sulfate attacks or protects the manganese in the binding site which is attacked by cholic acid.

The electron transfer rates indicate that while none of the samples bridged electron transfer from water to methyl viologen, inhibition of diphenylcarbazide to methyl viologen electron transfer is greatest in chloroplasts treated with cholic acid only. Inhibition by ammonium sulfate is not as great and it appears that the presence of ammonium sulfate offers some protection to the water oxidizing system from attack by cholic acid.

d) Signal II in the Cholate Pellet

1) Signal II

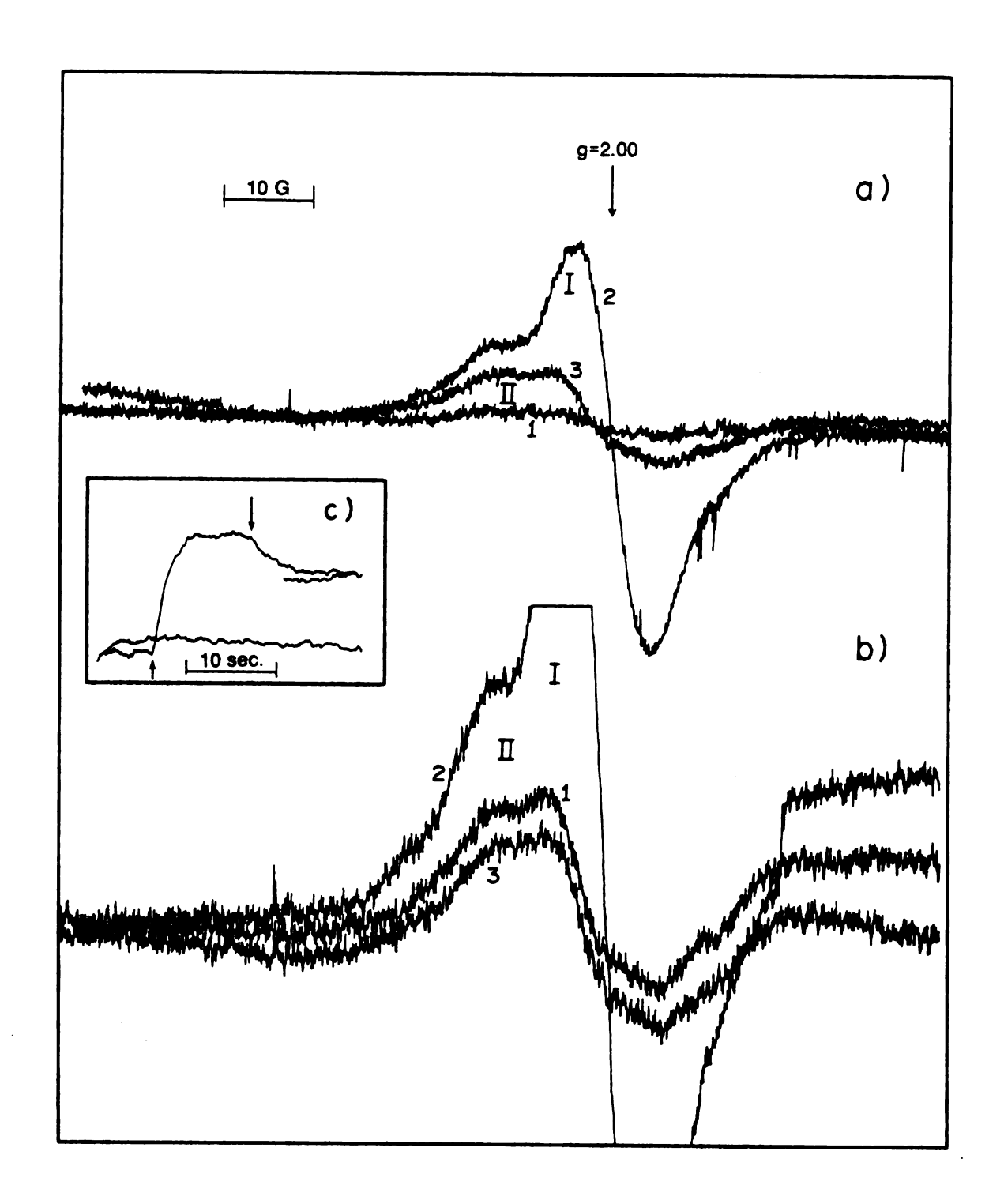
Light activation of Photosystem II forms a paramagnetic species which has a characterizatic EPR signal at g = 2.0043 called Signal II [22]. Babcock and Sauer and Blankenship et al. have shown that Signal II is composed of three components: Signals IIs (slow kinetics), IIf (fast kinetics) and IIvf (very fast kinetics) [23,24,25]. Signal IIf is produced in the light after washing with Tris

buffer, heating or treatment with chaotropic agents, all treatments which inhibit oxygen evolution [23]. The signal power saturates at 20 mW. It exists in a one to one ratio with Signal I (P700 in Figure 1). It has been proposed that Signal IIf arises from Z^{\ddagger} , the oxidized physiological donor to P680 (see Figure 1) [24]. In oxygen evolving chloroplasts the oxidation of Z and its rereduction by the water splitting system are fast enough that Signal IIf is not observed and Z^{\ddagger} gives rise to the fast decaying transient, which is referred to under these conditions as Signal IIvf [25]. Only upon inhibition of oxygen evolution does Z remain in its paramagnetic state, Z^{\ddagger} , long enough to be observed by EPR as Signal IIf.

It would be of interest to observe Signal II in the pellet obtained after treatment with cholic and ammonium sulfate to see if Z is removed from the membrane by the treatment. Figure 12 shows that the light-induced Signal II component found in the cholate pellet has the same characteristics as reported by Babcock and Sauer for Signal IIf [24]. Figure 12a shows that in the dark (1) the level of Signal II is very low. In the light the signal increases (2). In the dark following illumination, the level of the signal is about half that seen in the light (3). Figure 12b is essentially the same experiment as Figure 12a at a higher instrument gain setting and using a preilluminated sample. In the preilluminated

Figure 12 (a) Signal II in the cholate pellet. (1) dark. (2) light. (3) dark after light. Instrument settings:
Field, 3390 G; Field width, 100 G; Modulation amplitude,
5 G; Time constant, 0.1 sec; Scan time, 4 min; Power, 20 mW;
Frequency, 9.45 GHz; Gain, 4 × 10³; [chl] 5.57 mg/ml.
(b) Same sample as in (a). (1) dark after light. (2)
reilluminated. (3) dark. Instrument settings: same as
for (a) except time constant, 0.3 sec; Scan time, 8 min;
Gain, 1.25 × 10⁴. (c) Instrument settings adjusted to observe the light induced changes at the top of Signal II. Instrument settings: Field, 3383 G; Field width, 0; Modulation amplitude 5 G; Time constant, 1 sec; Scan time, 30 sec; Frequency
9.45 GHz; Gain, 3.2 × 10⁴; Power, 20 mW; Arrow up, light on.

Arrow down, light off.



sample there is a signal present (1) which doubles upon illumination (2) and drops back down when returned to the dark (3). The slow decaying signal in (1) and (3) is Signal IIs and the signal in (2) is Signal IIf. The insert of Figure 12 shows light induced changes in the signal monitored at the low-field peak of Signal II (at the field strength labelled II in figure 12a). Note that the instrument gain is eight times that in Figure 12a. When the light is turned on (arrow up) there is a rapid rise of the signal; when the light is turned off (arrow down) the signal drops to about half the light on value showing again the presence of the slow decaying Signal IIs.

2) Microwave Power Saturation

The microwave power saturation profile of a radical can be informative about the environment of the unpaired electron [26]. The application of a magnetic field to a paramagnetic species induces a population difference in the ground and excited states of the unpaired electron through absorption of energy according to the resonance equation $h\nu = g\beta H$. This population difference and energy absorption result in the observed EPR spectrum. The spin system relaxes by releasing energy to the lattice system surrounding it. As energy is put into the spin system at a faster rate, electronic transitions occur more often (while the population difference remains constant) and the EPR signal increases. As long as the rate of energy release to the lattice is greater than the rate of energy absorption

from the microwave power field, the EPR signal will increase with increasing microwave power. When the rate of energy into the spin system is greater than the rate at which energy is released to the lattice, the increase of energy into the spin system causes the population difference between the ground and excited states to decrease. Fewer transitions will then be able to occur and the EPR signal will decrease. This situation is referred to as power saturation.

Signals IIs and IIf power saturate at about 20 mW [27]. Signal IIvf does not power saturate at 200 mW [27]. It has recently been found that in chloroplasts treated with NH3, no power saturation of Signal II is observed [40]. Power saturation at 50 mW is observed for Tris washed chloroplasts and at 20 mW for chloroplasts treated with Tris and 50 mM Ca²⁺ [40]. These observations indicate that the manganese associated with water oxidation facilitates spin-lattice interaction for Signal II leading to saturation at higher power levels. Treatments that loosen or release Mn²⁺ from its binding site cause by this release a lowering of the power saturation level.

Figure 13 shows the saturation profile of Signal II found in the cholate pellet in the form of a plot of signal amplitude vs. (power) . The signal saturates at 20 mW indicating that the manganese which is associated with Signal II has been perturbed from its binding site by the cholic acid treatment.

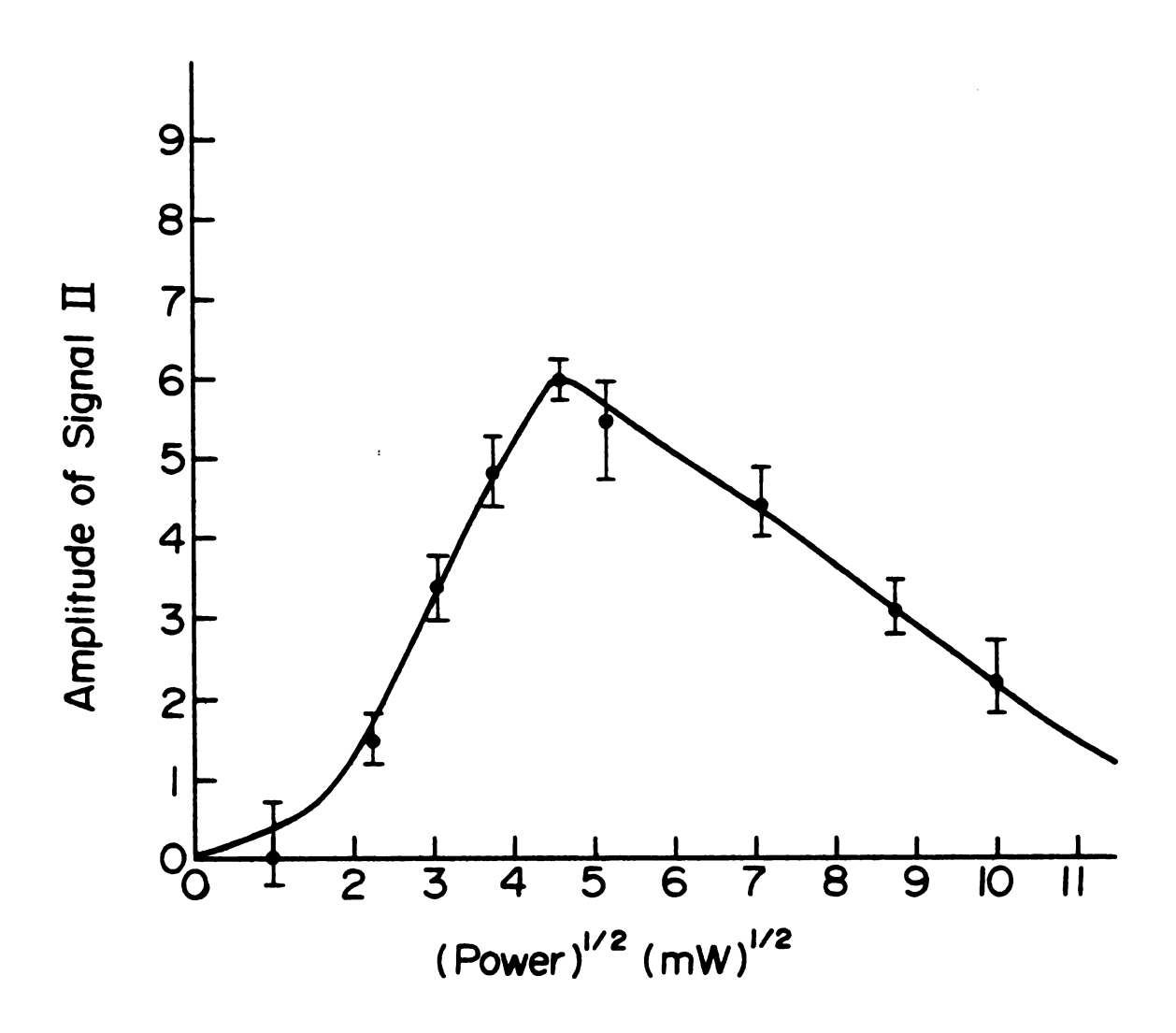


Figure 13. Microwave power saturation of Signal II in the cholate pellet. Instrument settings: Field, 3390 G; Field width, 100 G; Modulation amplitude, 5 G; Time constant, 0.3 sec; Scan time, 8 min; Frequency, 9.45 GHz; Gain, 1.25×10^4 .

D. CONCLUSIONS

The 65 kDalton protein isolated by Spector and Winget is reported to contain two manganese atoms [20]. The data in Table 1 indicate that of 5 Mn/400 chl contained in functional chloroplasts, 4 Mn/400 chl remain in the membrane-containing pellet obtained by centrifugation after treatment with cholic acid and ammonium sulfate. Only one manganese per reaction center is released into the supernatant. The data also show that of the manganese released into the supernatant, nearly half of it is not bound to any protein so that it is EPR-detectable. If the protein isolated by Spector and Winget from the supernatant contained two manganese atoms, the protein must have become associated with the manganese after the cholic acid treatment.

With the observation of Signal IIf in the pellet, we have shown that Z, the intermediary between P680 and the water oxidizing complex, remains in the membrane after extraction by cholic acid and ammonium sulfate. The power saturation curve of Signal II indicates that the manganese associated with Signal II is perturbed from its binding site. It is not clear if this manganese is removed from the membrane or only removed from its binding site in the

membrane enough to restrict its action in the spin-lattice relaxation mechanism for Signal II. Treatments which inhibit oxygen evolution result in the observation of the properties of Signal II reported here. These observations, together with the fact that only a small amount of manganese is found in the supernatant, raise the possibility that the manganese released into the supernatant after treatment with cholic acid and ammonium sulfate is not essential to water oxidation and that oxygen evolution is inhibited through disruption of the action of the essential manganese left in the membrane. The inability to restore water oxidation activity by washing the pellet with buffer and the data in Table 2 indicate that inhibition is not accomplished only by the ammonium sulfate; cholic acid also plays a role in the inhibition of oxygen evolution.

Previously it has been reported that hydroxylamine can act as an electron donor to Photosystem II in chloroplasts in which water oxidation has been inhibited by ammonia [35]. Results obtained by using hydroxylamine as an electron donor to Photosystem II cannot be reliably generalized to other electron donors because hydroxylamine is itself an inhibitor of water oxidation. The data in Table 2 show that diphenylcarbazide can act as an electron donor to Photosystem II in chloroplasts in which water oxidation has been inhibited by ammonia at high concentration (0.4 M (NH₄)₂SO₄ (pH 8.0)). The results

obtained using DPC as electron donor can be generalized to other electron donors. Electron flow in chloroplasts which has been interrupted through inhibition of water oxidation by ammonia can be restored by the addition of exogenous electron donors.

The data collected in this thesis also add support to the idea that there is more than one pool of manganese in the water oxidation center. That is, the separate manganese atoms may perform different functions in the water oxidation process. This is supported by data which show that different treatments have different effects on the manganese present. Cholic acid releases one Mn²⁺ from the membrane and makes one more, which remains with the pellet after centrifugation, detectable by EPR.

Treatment of the pellet with NH₂OH and 50 mM Ca²⁺ releases two more Mn²⁺; 0.8 M Tris causes the release of one more Mn²⁺ in the pellet. These different responses to these treatments indicate that further investigation into the idea of separate functions for the manganese involved in water oxidation is warranted.

LIST OF REFERENCES

LIST OF REFERENCES

- [1] Ruben, S., Randall, M., Kamen, M., Hyde, J.: J. Amer. Chem. Soc., 63, 877-879 (1941).
- [2] Radmer, R., Cheniae, G.: in <u>Primary Processes of Photosynthesis</u> (J. Barber, ed.), pp. 303-345, Elsevier, Amsterdam (1977).
- [3] Kok, B., Forbush, B., McGloin, M.: Photochem. Photobiol., 11, 457-475 (1970).
- [4] Joliot, P., Barbieri, G., Chabaud, R.: Photochem. Photobiol., 10, 390-329 (1969).
- [5] Fowler, C.F.: Biochim. Biophys. Acta, 462, 414-421 (1977).
- [6] Cheniae, G.M., Martin, I.F.: Brookhauer Symp. Biol., 19, 406-417 (1966).
- [7] Cheniae, G.M., Martin, I.F.: Plant Physiol., <u>47</u>, 568-565 (1971).
- [8] Yocum, C.F., Yerkes, C.T., Blankenship, R.E., Sharp, R.R., Babcock, G.T.: Proc. Nat. Acad. Sci. manuscript submitted.
- [9] Robinson, H.H., Sharp, R.R., Yocum, C.F.: Biochim. Biophys. Res. Comm., 93, 755-761 (1980).
- [10] Velthuys, B.R.: Biochim. Biophys. Acta, 396, 392-401 (1975).
- [11] Joliot, A.: Biochim. Biophys. Acta, <u>126</u>, 587-590 (1966).
- [12] Sharp, R.R., Yocum, C.F.: Biochim. Biophys. Acta, 635, 90-104 (1981).
- [13] Bouges, B.: Biochim. Biophys. Acta, 234, 103-112 (1971).
- [14] Cheniae, G.M., Martin, I.F.: Plant Physiol., <u>50</u> 87-94 (1972).

- [15] Cheniae, G.M., Martin, I.F.: Biochim. Biophys. Acta, 502, 321-344 (1978).
- [16] Theg, S.M., Sayre, R.T.: Plant Science Letters, <u>16</u>, 319-326 (1979).
- [17] Sharp, R.R., Yocum, C.F.: Biochim. Biophys. Acta, 592, 185-195 (1980).
- [18] Blankenship, R.: Ph.D. Thesis, Univ. of California at Berkeley (1975).
- [19] Wertz, J., Bolton, J.: <u>Electron Spin Resonance</u>: <u>Elementary Theory and Practical Applications</u>, McGraw-Hill, New York (1972).
- [20] Spector, M., Winget, D.: Proc. Nat. Acad. Sci., <u>77</u>, 957-959 (1980).
- [21] Sun, A., Sauer, K.: Biochim. Biophys. Acta, 234, 399-414 (1971).
- [22] Commoner, B., Heise, J., Lippinott, B., Norbert, R., Passonen, J., Townsend, J.: Science, 126, 57-63 (1957).
- [23] Babcock, G.T., Sauer, K.: Biochim. Biophys. Acta, 325, 483-503 (1973).
- [24] Babcock, G.T., Sauer, K.: Biochim. Biophys. Acta, 376, 315-328 (1975).
- [25] Blankenship, R.E., Babcock, G.T., Warden, J.T., Sauer, K.: FEBS Letts., 51, 287-293 (1975).
- [26] Bolton, J. in <u>Biological Applications of Electron Spin</u>
 Resonance, (Swartz, H., Bolton, J., Berg, D., eds.) pp.
 11-61, Wiley-Interscience, New York (1972).
- [27] Warden, J., Blankenship, R., Sauer, K.: Biochim. Biophys. Acta, 423, 462-478 (1976).
- [28] Reed, G.H., Leigh, J.S., Pearson, J.E.: J. Chem. Phys., <u>55</u>, 3311-3316 (1971).
- [29] Hudson, A., Luckhurst, G.R.: Mol. Phys., <u>16</u>, 395-403 (1969).
- [30] Hinckley, C.C., Morgan, L.O.: J. Chem. Phys., 44, 898-905 (1966).
- [31] Dismukes, C.G., Siderer, Y.: Proc. Nat. Acad. Sci. USA, 78, 274-278 (1981).

- [32] Yerkes, C.T.: Masters Thesis, Michigan State Univ. (1979).
- [33] Ochiai, E.: <u>Bioinorganic Chemistry</u>, An Introduction, p. 388, Allyn and Bacon, Inc., Boston, MA (1977).
- [34] Saphon, S., Crofts, A.R.: Z. Naturforsch, <u>32c</u>, 617-626 (1977).
- [35] Izawa, S., Heath, R.L., Hind, G.: Biochim. Biophys. Acta, 180, 388-395 (1969).
- [36] Kelly, P.M., Izawa, S.: Biochim. Biophys. Acta, 502, 198-210 (1978).
- [37] Muallem, A., Izawa, S.: FEBS Lett., <u>115</u>, 49-53 (1980).
- [38] Clayton, R.K.: <u>Photosynthesis</u>: <u>Physical Mechanisms</u> and <u>Chemical Patterns</u>, p. 204, Cambridge Univ. Press (1980).
- [39] Wydryzynski, T., Sauer, K.: Biochim. Biophys. Acta, 589, 56-70 (1980).
- [40] Yocum, C.F., Babcock, G.T.: FEBS Lett., manuscript submitted.
- [41] Williams, W.P. in <u>Primary Processes of Photosynthesis</u> (J. Barber, Ed.), p. 101-147, Elsevier, Amsterdam (1977).
- [42] Frasch, W.D., Cheniae, G.M.: Plant Physiol., <u>65</u>, 735-745 (1980).